



Norwegian  
Meteorological  
Institute

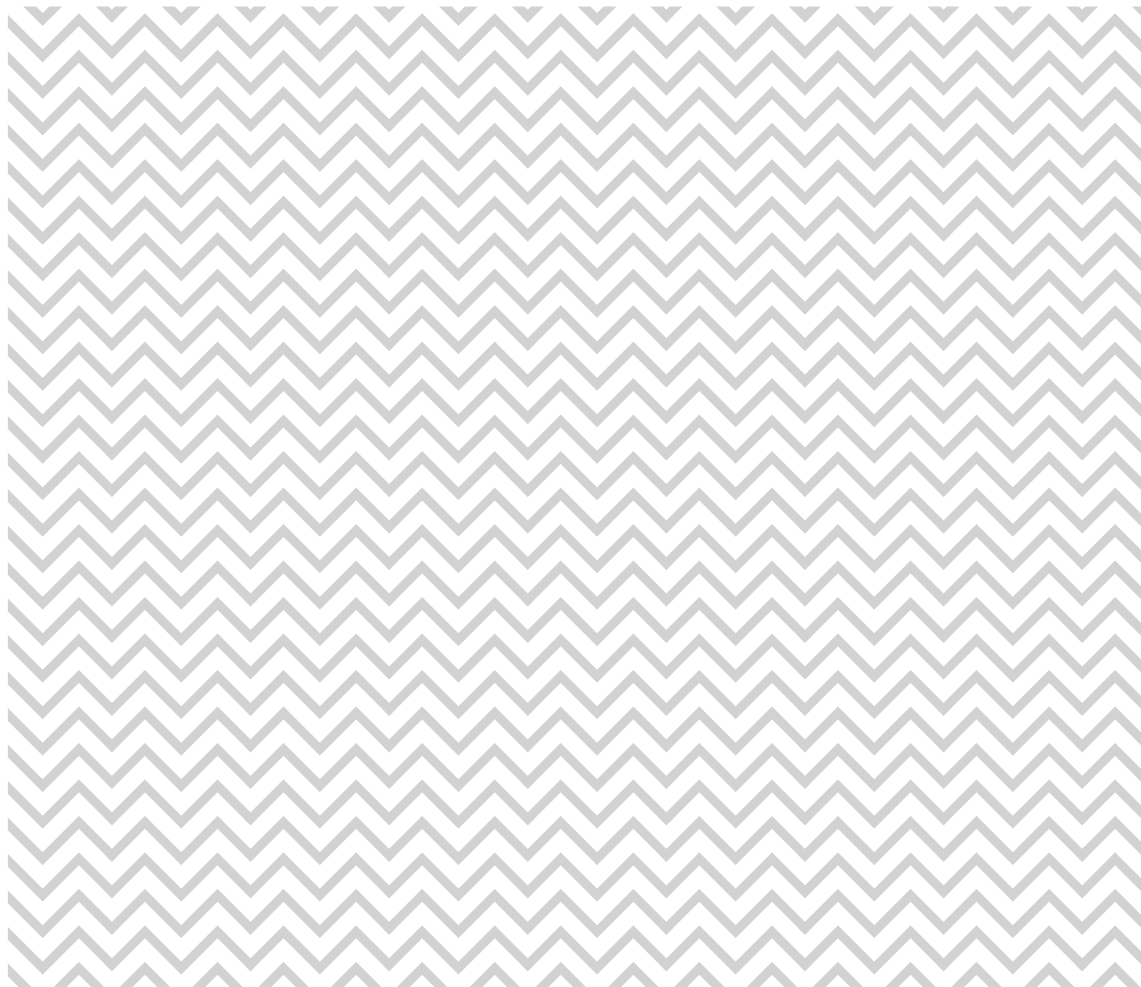
no. 2/2015  
ISSN 2387-4201  
Numerical Weather  
Prediction

## **MET report**

# **The impact of ASCAT winds in storm cases using the HARMONIE model system**

**EUMETSAT Fellowship Programme: First year report**

Teresa Valkonen and Harald Schyberg







Norwegian  
Meteorological  
Institute

## MET report

<b>Title</b> The impact of ASCAT winds in storm cases using the HARMONIE model system	<b>Date</b> January 27, 2015
<b>Section</b> Numerical Weather Prediction	<b>Report no.</b> 2/2015 ISSN 2387-4201
<b>Author(s)</b> Teresa Valkonen and Harald Schyberg	<b>Classification</b> <input checked="" type="radio"/> Free <input type="radio"/> Restricted
<b>Client(s)</b> EUMETSAT, MET Norway	<b>Client's reference</b>
<b>Abstract</b> Scatterometer winds have a potential to improve forecasting of severe weather events by improving the initial state of atmosphere through data assimilation. Within the EUMETSAT fellowship project, Advanced Scatterometer (ASCAT) ocean surface wind data from MetOp-A and MetOp-B satellites are applied in the 3D-Var data assimilation system available in the high-resolution HARMONIE model used at the Norwegian Meteorological Institute. The ASCAT wind data assimilation demonstrates a slight positive impact on forecasting mean sea level pressure (MSLP) at the forecast lengths of 3-21 hours for a selected severe storm case. Upper levels show a slight improvement on the 24-h forecast of wind speed at 850 hPa, temperature at 700 hPa and specific humidity at 500 hPa. Other surface variables or the upper atmosphere do not experience significant changes. The first attempt to optimise the use of ASCAT data by reducing the thinning distance further improves the average verification scores slightly for MSLP. The reduced thinning distance applied in a polar low case clearly improves the MSLP at the time of the polar low event, even though ASCAT data do not enhance the statistics averaged over the whole simulation period in this case. This limited set of experiments were cases where we found data assimilation of ASCAT to be beneficial for forecasting of storms.	
<b>Keywords</b> data assimilation, numerical weather prediction, scatterometry, ocean surface winds	

---

Disciplinary signature  
Jørn Kristiansen

---

Responsible signature  
Øystein Hov

Meteorologisk institutt  
Meteorological Institute  
Org.no 971274042  
post@met.no

Oslo  
P.O. Box 43 Blindern  
0313 Oslo, Norway  
T. +47 22 96 30 00

Bergen  
Allégaten 70  
5007 Bergen, Norway  
T. +47 55 23 66 00

Tromsø  
P.O. Box 6314  
9293 Tromsø, Norway  
T. +47 77 62 13 00

[www.met.no](http://www.met.no)  
[www.yr.no](http://www.yr.no)



# Contents

<b>1</b>	<b>Introduction</b>	<b>1</b>
<b>2</b>	<b>ASCAT ocean surface winds</b>	<b>2</b>
<b>3</b>	<b>Model experiments</b>	<b>3</b>
3.1	The HARMONIE model and assimilation system . . . . .	3
3.2	Assimilation of scatterometer winds . . . . .	5
3.3	Severe and high impact weather cases . . . . .	6
<b>4</b>	<b>Observation usage</b>	<b>8</b>
4.1	Data coverage . . . . .	8
4.2	Comparison with model background . . . . .	8
<b>5</b>	<b>Impact of ASCAT data assimilation on the forecast over land</b>	<b>14</b>
5.1	Surface variables . . . . .	14
5.2	Upper air fields . . . . .	17
<b>6</b>	<b>Test on the reduced thinning distance</b>	<b>21</b>
<b>7</b>	<b>Conclusions and outlook</b>	<b>25</b>
	<b>Acknowledgements</b>	<b>26</b>
	<b>References</b>	<b>29</b>
	<b>Appendix: List of abbreviations and acronyms</b>	<b>30</b>



# 1 Introduction

Rapidly developing storms with strong winds and associated other severe conditions can cause large damage when hitting the land in Europe. Forecasting these storms relies strongly on numerical weather prediction (NWP) models. Successful NWP forecasts are dependent on an accurate description of the atmospheric initial state in the model. Scatterometer winds provide detailed information on wind speed and direction in different stages of these storms over the ocean surface, and can help to improve the model initial state through data assimilation methods.

Several weather forecasting centres apply successfully scatterometer wind data assimilation in their global NWP models (ECMWF, *De Chiara et al.* 2012; Météo-France, *Payan* 2012; UK Met Office, *Cotton* 2013). Positive impacts have been reported also from limited area models, such as from the High Resolution Limited Area Model (HIRLAM), (e.g., *de Haan et al.*, 2013; *Ollinaho*, 2010; *Tveter*, 2006). Despite the possibility to use scatterometer winds in the model system of the Hirlam Aladin Regional/Mesocale Operational NWP In Europe (HARMONIE), the scatterometer wind assimilation is not operationally applied at the Norwegian Meteorological Institute (MET Norway), or at any other national weather service applying the same model.

The fellowship project *Scatterometer winds in rapidly developing storms* (SCARASTO) of the European Organisation for the Exploitation of Meteorological Satellites (EUMETSAT) aims to take better benefit of scatterometer winds in situations of rapidly developing storms. The fellowship work gains preliminary experience needed to progress towards the operational use of scatterometer winds in Norway using the HARMONIE model system. The gained experience on the assimilation system will serve as a baseline for further experimentation for finding optimal techniques to obtain the best beneficial impact of scatterometer data on forecasts of storm developments.

This report describes the knowledge gained during the first year of the fellowship. The Advanced Scatterometer (ASCAT) ocean surface wind data are applied in the three-dimension variational (3D-Var) data assimilation system available in the HARMONIE system used at MET Norway. Quality and coverage of scatterometer wind data, and impact on forecast performance are studied. Specifically, the aim of this first year report is to

- acquire skills in the implementation and available settings of scatterometer assimilation in the HARMONIE model system,
- investigate the temporal and spatial scatterometer data usage in the operational model system,
- learn about observation and model background accuracies by monitoring the scatterometer departures from the model background, and
- investigate the impact of scatterometer wind assimilation on the forecasts over land in a storm case.

Based on the results, the first attempt to optimise the use of ASCAT winds is done by reducing the thinning distance. The reduced thinning distance is then applied into a case with many polar lows during a short period of time.

## 2 ASCAT ocean surface winds

ASCAT is an active microwave instrument on-board satellite MetOp-A and MetOp-B, launched on 19 October 2006 and on 17 September 2012, respectively, by the European Space Agency (ESA) and operated by the EUMETSAT. The ASCAT instrument was designed to measure wind speed and wind direction over the oceans (*Figa-Saldaña et al.*, 2002). It operates on so called C-band with the microwave frequency of 5.255 GHz. The ASCAT instrumentation consists of three vertically polarised fan beams looking on each side of the satellite track. The ASCAT instrumentation system thus covers two approximately 550 km-wide swaths, which are separated by 670 km. Each swath provides measurements of radar backscatter from the ocean surface on a 25 km or 12.5 km grid divided into 21 or 41 so-called Wind Vector Cells (WVC). The orbit period of both satellites is approximately 90 minutes. The paths of MetOp-A and MetOp-B partly collocate for most latitudes, and they are 50 minutes apart in time.

The scatterometer wind retrieval is based on the presence of the wind-induced gravity-capillary waves on the water surface (*Stoffelen*, 1998). The gravity-capillary waves, with wavelength of some centimetres, respond very rapidly to the wind speed over the ocean surface. Radar backscattering from the ocean surface is governed by Bragg scattering (*Ulaby et al.*, 1982), which occurs from the gravity-capillary waves that are in resonance with the radar microwaves. Near-surface wind speed and direction can be determined from the three normalised radar cross section (NRCS or  $\sigma^o$ ) measurements from the antenna beams. The three  $\sigma^o$  measurements, also called triplets, are distributed on a cone when visualised in three dimensions. The cone is described by an empirically derived Geophysical Model Function (GMF) (*Hersbach et al.*, 2007; *Verhoef et al.*, 2008). The GMF thus describes the relation of the backscatter measurements to the mean wind vector in the WVC. In the wind retrieval process, the attempt is to find the wind speed and direction associated with the GMF backscatter triplet that is closest to the measured backscatter.

The ASCAT wind retrieval leads to 2–4 different wind solutions, called ambiguities (*Lin et al.*, 2013). The ambiguities are ranked by their probability or distance of measured backscatter triplet to the GMF cone. The distance to the cone is also known as inversion residual and Maximum Likelihood Estimator (MLE). Retrieved wind solutions are ranked in order. The first ranked solution corresponds to the lowest MLE value and has the highest probability to be true. The MLE value is also a good indicator of the retrieved wind quality.

The unambiguous stand-alone wind field is produced by applying an ambiguity removal (AR) scheme. A two-dimensional variational ambiguity removal technique (2D-

Var) is used for ASCAT (Vogelzang *et al.*, 2009). The AR scheme produces an analysis based on the ambiguous scatterometer wind solutions and a NWP model forecast. The solution closest to the analysis is selected. The 2D-Var product wind is usually used for weather monitoring and nowcasting where as wind ambiguities are applied in NWP data assimilation.

The Ocean and Sea Ice Satellite Application Facility (OSI SAF) of EUMETSAT processes the wind products from the calibrated backscatter products. This is known as ASCAT level 2 processing. The Royal Netherlands Meteorological Institute (KNMI) is responsible for production, development, and distribution of the OSI SAF ASCAT wind products. There are five different ASCAT scatterometer wind products available through OSI SAF and the EUMETSAT Advanced Retransmission Service (EARS) (*ASCAT Wind Product User Manual*, 2013). As the ASCAT 12.5-km product contains more small details than the 25-km product (Vogelzang *et al.*, 2011), the global OSI SAF coastal wind product with 12.5-km spacing is used in this work. The data are obtained through the KNMI server. Data from both the MetOp-A and MetOp-B satellites are utilised.

The accuracy of ASCAT products is characterised by a wind component root-mean-square error smaller than 2 m/s and a bias of less than 0.5 m/s in wind speed compared to buoy observations and ECMWF NWP data, as described in *ASCAT Wind Product User Manual* (2013). The quality of the ASCAT products have also been assessed for accuracy and resolution using spectral analysis and so called triple collocation with buoy measurements and NWP model forecasts (Vogelzang *et al.*, 2011; Verspeek *et al.*, 2013a,b). Vogelzang *et al.* (2011) conclude that the triple collocation error standard deviations of the scatterometer winds are approximately 1 m/s or better with respect to the scales resolved by the scatterometer wind products. Buoy collocations and triple collocation also show that there are no significant differences in wind quality between the ASCAT wind products from the MetOp-A satellite and the MetOp-B satellite (Verspeek *et al.*, 2013b).

## **3 Model experiments**

### **3.1 The HARMONIE model and assimilation system**

The model experiments described here make use of the HARMONIE model system, version 37h1.2 which was the operational model version at MET Norway at the time. The HARMONIE is a non-hydrostatic convective scale NWP model system. It is used, maintained and developed within the HIRLAM programme which consists of national weather services of the five Nordic countries, Netherlands, Ireland, Spain, Estonia and Lithuania. The HARMONIE model code is developed in a cooperation with ECMWF, Météo-France and its collaborative weather services in central and eastern Europe and northern Africa within a consortium called ALADIN (Aire Limitée Adaptation dynamique Développement InterNational). Météo-France and the ALADIN have had a major initial contribution to the model code of HARMONIE, and the default setting of HARMONIE with 2.5 km grid spacing is very close to the AROME model of Météo-France (Seity *et al.*, 2011).

The HARMONIE model has non-hydrostatic spectral dynamics based on semi-implicit semi-Lagrangian discretisation using hybrid vertical coordinates. Physical processes smaller than grid size are parametrised. Longwave radiation makes use of the Rapid Radiative Transfer Model (RRTM) code (*Mlawer et al.*, 1997), and shortwave radiation is based on the old scheme of the ECMWF model (*Morcrette and Fouquart*, 1986). Turbulence is parametrised applying the 1D prognostic Cuxart-Bougeault TKE scheme (*Cuxart et al.*, 2000). The ICE3 package is used for the description of the micro-physics of clouds (*Pinty and Jabouille*, 1998). Shallow convection parametrisation makes use of a combined eddy diffusivity- mass-flux scheme (EDMF-M, *de Rooy and Pier Siebesma*, 2010). Surface and soil processes are described with a separate surface model SURFEX (SURFace EXternalisee) which distinguishes between different surface types and consists of a scheme for each (*Masson et al.*, 2013).

The upper air data assimilation in HARMONIE is based on a 3D-Var system described by *Brousseau et al.* (2011). Additionally, there is an option to blend the 3-hour HARMONIE forecast with the large scale structures from the ECMWF forecast to obtain the background field (*Dahlgren*, 2013). The option was tested but turned off in the results presented in this report. Background error statistics are derived using the ensemble method where the model errors are estimated by the differences of 6h-forecasts initialised by the ensemble of analysis from the ECMWF ensemble prediction system. One winter month (January 2012) and one summer month (July 2012) with four ensembles twice a day are used for the current statistics. The multivariate formulation (*Derber and Bouttier*, 1999; *Berre*, 2000) is used for deriving the background error covariances from the forecast differences.

The default conventional observations to be assimilated into the system are surface observations from synoptic station (SYNOP), ships (SHIP), and drifting buoys (DRIBU), and upper air observations from radiosoundings (TEMP) and aircraft reports (AMDAR and AIREP). The variables assimilated are summarised in Table 1. In addition, it is possible to assimilate different types of remote sensing data into the HARMONIE model system. The observation types currently or in near future available for assimilation are advanced microwave sounding unit (AMSU) radiances, radar reflectivity and wind, global navigation satellite system (GNSS) data, infrared atmospheric sounding interferometer (IASI), and atmospheric motion vectors (AMV). The different data types might affect the quality of the forecast differently, and investigating the sensitivity of ASCAT winds in the presence of other observation types is important in the future. It is expected that the impact of one observing system is smaller when additional above mentioned observing systems are included. At this stage, however, the ASCAT data were the only satellite data type used in the data assimilation in this work.

Data assimilation of surface variables in the HARMONIE system is based on optimal interpolation. It is done by applying a module called CANARI (Code d'Analyse Nécessaire à Arpege pour ses Rejets et son Initialisation, *Taillefer*, 2002) which do the analysis of the screen level parameters (2-m temperature and 2-m relative humidity) and snow depth. In addition to the horizontal analysis, 2-m-analysis increments are vertically propagated

Table 1: The default conventional observations assimilated into the 3D-Var system of HARMONIE.  $z$  stands for geopotential height,  $u$  zonal wind component,  $v$  meridional wind component,  $T$  temperature, and  $q$  specific humidity.

	Observation type	Variables used
Surface	SYNOP	$z$
	SHIP	$u, v, z$
	DRIBU	$z$
Upper air	TEMP	$u, v, T, q$
	AMDAR/AIREP	$u, v, T$

to the soil temperature and water by empirically derived coefficients.

### 3.2 Assimilation of scatterometer winds

In the HARMONIE model system, data assimilation of scatterometer winds relies on the wind retrieval products of OSI SAF, and no wind inversion is done as a part of the HARMONIE system. The data assimilation of ASCAT winds, and any data type, consists of three parts. First, the observation data are read into the data base. Then, the appropriate data to be used are selected. Finally, the selected data are used in the data assimilation.

The ASCAT data are read into the HARMONIE model system with a programme called Bator. Bator is the pre-processing step which creates the observation data base (ODB) for the data assimilation. The assimilation window length is 3 hours in this study. Because the First Guess at Appropriate Time (FGAT) scheme is not available in the HARMONIE system, the window length of 3 hours means that any ASCAT data  $\pm 1.5$  h the analysis time are handled as if they had taken place at the analysis nominal time. The ASCAT data latency was not taken into account in this work.

After getting ASCAT data into the ODB, the next step is screening for observations suitable for data assimilation. The quality control includes blacklisting data, data selection by quality flags and model background check. ASCAT data over land and sea-ice are rejected as well as wind speeds over 35 m/s. On the accepted observations, data thinning is applied. The thinning is done in order to avoid spatially correlated errors or representativeness errors in the satellite observations as the 3D-Var data assimilation is based on the assumption of uncorrelated observation errors. By the default settings, the thinning distance is approximately 100 km.

The selected observations enter the actual data assimilation. The purpose of the 3D-Var data assimilation is to find the best estimate for the true atmospheric state  $\mathbf{x}$ . That is done by minimisation of the cost function  $J$ .

$$J(\mathbf{x}) = J_b + J_o = \frac{1}{2}(\mathbf{x} - \mathbf{x}_b)^T (\mathbf{B})^{-1} (\mathbf{x} - \mathbf{x}_b) + \frac{1}{2}[\mathbf{y}_o - H(\mathbf{x})]^T \mathbf{R}^{-1} [\mathbf{y}_o - H(\mathbf{x})] \quad (1)$$

where  $J_b$  is the cost function for the background and  $J_o$  the cost function for the observations,  $x_b$  is the background,  $\mathbf{B}$  and  $\mathbf{R}$  are the background and observations covariance matrices,  $y_o$  observations and  $H$  represents the observation operators. The minimisation in the HARMONIE model system is done by M1QN3 minimiser (*Gilbert and Lemaréchal, 1989*).

The cost function of observations  $J_o$  is a sum of cost functions of individual observation types, such as

$$J_o = J_{o,SYNOPT} + J_{o,ASCAT}\dots \quad (2)$$

For ASCAT, two ambiguous wind solutions are considered in the 3D-Var. De-aliasing of the wind solutions is done during the assimilation processing. The most appropriate wind solution is selected for assimilation by comparison with the HARMONIE winds. The other wind solution is rejected and not used in the minimisation. For the selected ASCAT wind solution, the observation error for zonal wind  $u$  and meridional wind  $v$  components are set to 2.0 m/s. ASCAT winds are assimilated as components of 10-m neutral wind. Observation operator for ASCAT describes the connection between the equivalent model neutral wind at 10 m height at the observation location and the model wind at the lowest model level (*Payan, 2010*). This is done by using a surface scheme based on the Monin-Obukhov formulations. The  $\mathbf{B}$  matrix expresses the correlations for each model level with the others, and spreads the information of ASCAT winds to the upper levels.

### 3.3 Severe and high impact weather cases

The focus of the SCARASTO project is on weather systems with rapid or unexpected development, strong winds or large damage potential. This includes both synoptic-scale mid-latitude cyclones and small-scale and short-lived low pressure systems, such as polar lows.

The list of severe weather events serves as a basis for experimentation and case studies with ASCAT winds. MET Norway operates a national warning system for severe weather events (*Plan for varsling av ekstreme værforhold, 2014*). A severe weather warning is to be sent when it is likely that weather will cause comprehensive damage or danger to human life and property in a considerable land area. The warning system includes the following phenomena: strong winds, large precipitation amounts, avalanche, storm surge and waves, or combination of them. There has been 64 severe weather events in Norway since 8 December 1994 when the warning system begun its operation. After severe events, cases are archived and reports are written by duty forecasters at MET Norway for internal and external use. Most of the severe events have been related to strong cyclones, which have reached Norway from the Atlantic.

The first case to experiment with ASCAT data was a mid-latitude cyclone that hit the Norwegian coast on 16 November 2013. The cyclone, named Hilde, was considered severe and one of the strongest reported in Norway (*Ekstremvêrrapport, 2013*). The model experiments for the period 11/11/2013 – 18/11/2013 were made applying the HARMONIE system. The main experiment (Hilde-ASCAT) included data assimilation of conventional

Table 2: Summary of performed experiments

Case	Period	Experiment name	Data assimilated	Thinning distance
Hilde	11/11/2013 – 18/11/2013	Hilde-CONV	CONV	-
		Hilde-ASCAT	CONV, ASCAT	100 km
		Hilde-ASCATthinn	CONV, ASCAT	50 km
Polar low	01/03/2013 – 08/03/2013	PL-CONV	CONV	-
		PL-ASCATthinn	CONV, ASCAT	50 km

observations and ASCAT winds, and the control one (Hilde-CONV) only conventional observations. The first attempt to optimise the use of ASCAT winds was done by reducing the thinning distance to 50 km for the cyclone case (Hilde-ASCATthinn). Other settings, including observation weighting, were kept the same.

In addition to the above mentioned severe weather events, there are other weather systems with unexpected development, strong winds or damage potential, such as polar lows. Polar lows are small but intense small-scale cyclones, which occur after a cold air outbreak to the relatively warm open sea. They have a horizontal scale from 200 km up to 1000 km, and they always occur north of the major baroclinic zone. Surface winds are higher than 15 m/s (gale force). There are large variations in the annual occurrence, but on average there have found to be 12 polar low events per year in the forecasting regions of MET Norway (Noer *et al.*, 2011). Numerical forecasting of polar lows remains challenging mainly due to the small spatial and temporal scales, weaknesses in the description of physical processes in the model and inaccuracies of the model analysis over regions where polar lows originate from. Scatterometer winds can provide observational information of polar lows in different stages of their life time and it is therefore attempting to study the impact of ASCAT winds in a polar low case.

The experimental setup with reduced thinning distance was additionally applied to a polar low case that took place on 6 March 2013. The model simulation (PL-ASCATthinn) was again limited to one week, being 01/03/2013 – 08/03/2013. To study the impact of ASCAT data, a control experiment (PL-CONV) with only the conventional observations assimilated was performed.

The performed model experiments are summarised in Table 2. All experiments were performed with 2.5 km grid spacing on the operational model domain used in Norway, covering roughly Scandinavia, Finland and the Baltic states (Figure 1). The system was run with 3D-Var data-assimilation with 3-hourly assimilation cycle, each of them producing a forecast for 48 hours. The ECMWF forecasts with 1-h interval were used as lateral boundary conditions. The ECMWF computing facilities were utilised for computing. The first day of the experiment period was considered as a spin-up time for the model, and data from it was not taken into account on the statistics. The results from the severe

cyclone case with default settings (Hilde-ASCAT) are presented in Section 4 and Section 5. The results from experiments with reduced thinning distance both from the cyclone (Hilde-ASCATthinn) and the polar low case (PL-ASCATthinn) are presented in Section 6.

## 4 Observation usage

### 4.1 Data coverage

The available ASCAT data coverage in the domain varies a lot depending on the time of the day (Figure 2). The 3-hour assimilation window allows good spatial coverage within the domain on cycles 09 UTC, 12 UTC, 18UTC and 21UTC, though the ocean region in the domain is narrow and meteorological systems rapidly proceed over to the land. Night cycles (00-06 UTC) are not covered by ASCAT in the domain. As the nominal MetOp orbit repeat cycle is 29 days, there are some day-to-day variations in the swath locations and thus also in the number of data hitting the model domain. The daily variations are, however, rather small and the diurnal distribution of data amount in this study gives a good estimate of the data amount in the domain in general.

Approximately 1% of all available ASCAT data amount was used in the data assimilation. The main reason for data rejection is the thinning. Quality control based on the KNMI quality flags accounts for a small portion of rejection. In addition, cycles at 09UTC and 21UTC encountered problems where almost all data were rejected. The reason for the excessive data rejection on these cycles remains unclear. The system used was originally designed for 25 km ASCAT data from one satellite only. The next model versions are properly updated for use of two satellites and their use is advisable. When using observations from two satellites, the data are thinned together, and only one observation is selected in the common areas.

Figure 1a illustrates the ASCAT data usage over the domain when the severe storm had arrived into the model domain. The strong thinning and data rejection can be seen, as well as an individual ambiguity selection problem (around 65°N, 10°E), which is enlarged in Figure 1b. The found ambiguity selection problems were mostly related to proceeding fronts as the 3D-Var data assimilation system cannot make use of the time of observations. Gross error problems, for example due to heavy precipitation or instrumental technical issues, were not found in the assimilated ASCAT data during this study period, which indicates that the data rejection procedure works effectively.

### 4.2 Comparison with model background

Influence of adding ASCAT winds in the model system can be studied by comparing the model fit to the scatterometer observations. Figure 3 presents the frequency distributions of background and analysis departures for assimilated ASCAT winds. Biases of the background departures (-0.48 m/s for  $u$ , -0.07 m/s for  $v$ ) are somewhat typical but the mean standard deviations (STD; 2.3 m/s for  $u$ , 2.5 m/s for  $v$ ) are larger than typically reported for

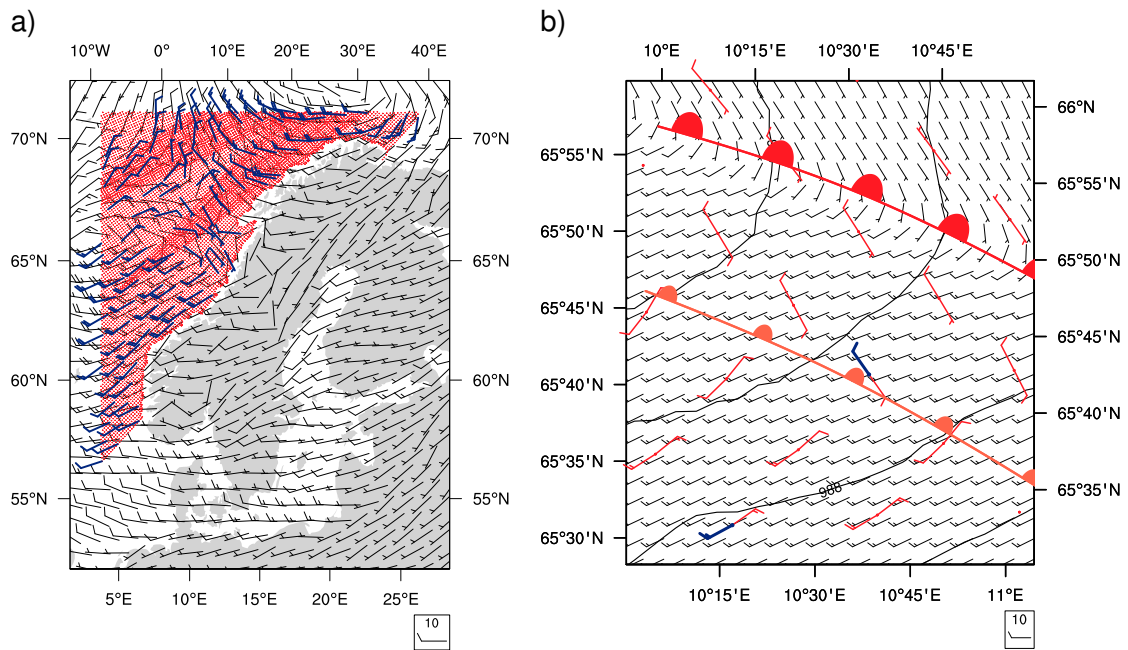


Figure 1: a) An example of ASCAT data coverage over the model domain at 16 November 2013 12 UTC cycle for the case Hilde-ASCAT. The red dots are the ASCAT data points, the blue wind barbs are the used ASCAT winds, and the black wind barbs are the background winds. b) An example of ambiguity selection problem near a front. The red wind barbs indicate the available ASCAT wind solutions (two ambiguities), the blue wind barb the selected and assimilated ASCAT wind solution, and the black wind barbs the background winds. The northern front (in red) illustrates the front location of the background field, and the southern front (in orange) the front location of the ASCAT observations.

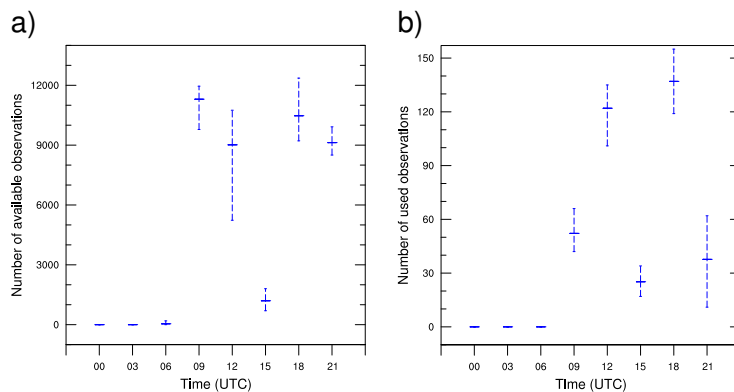


Figure 2: a) Number of ASCAT data points read into the model and b) number of ASCAT data points used in the data assimilation on each cycle for the case Hilde-ASCAT. The horizontal line marks the average number, and the vertical dashed bars the range for each model cycle.

ASCAT globally. Locally, however, the departures are known to be higher north from 60°N than in the lower latitudes (*C. Payan*, personal communication, January 2015). There is a reasonable reduction of departure biases and standard deviations in the analysis (bias -0.33 m/s for  $u$ , -0.02 m/s for  $v$ , and STD 1.7 m/s for  $u$ , 1.8 m/s for  $v$  in the analysis). The time series of departures (Figure 4) reveal strong day-to-day variations during the simulation period indicating that model fit to scatterometer observations is dependent on the atmospheric flow patterns.

One factor behind the relatively large departures between the ASCAT and the model background is the time difference between the observation measurement and the nominal analysis time. The 3-hour-long assimilation window generates ambiguity selection problems close to proceeding fronts. An example of this can be seen in Figure 1b. For that case, the ASCAT observations were made 44 minutes before the analysis time resulting in the placement difference of the warm front in the observations and the background field. The ASCAT wind solution, which was less likely to have occurred in reality, was selected for data assimilation because it was closer to the HARMONIE background field. The ambiguity selection problem rising from the observation timing could be reduced either by assimilating the 2D-Var product wind, for which the ambiguity removal is done with a time dependent data assimilation method, or by reducing the assimilation window. The former would have an increased risk of errors coming from the coarser resolution model and longer forecast ranges used for the ambiguity removal procedure. The latter would mean less observations used in the data assimilation but they would be more representative for the analysis time. In addition, it is attractive to do the ambiguity removal intrinsically in the HARMONIE 3D-Var system, where other observations are also available and will aid the ambiguity removal.

Figure 5 presents the model background departures for ASCAT winds which have entered the assimilation step (after screening and thinning) plotted by the time difference between the ASCAT measurement time and the analysis nominal time. This was done to see how much the departures suffer from the long assimilation window, and to learn more about the ambiguity removal in the data assimilation step. The wind speeds of the two wind solutions entering the data assimilation are about the same (Figure 5a). The selected wind solution is chosen by the wind direction, clearly seen in Figure 5b. This also confirms that the two first ranked ambiguities are about the same magnitude but 180 degrees from each other. ASCAT winds are not assimilated as wind speed and direction but as zonal and meridional wind components, which is why the background departures for selected wind components by the time difference are given in Figures 5c-5d. The large time differences between the measurement and analysis time are not consistently associated with large departures. However, if the assimilation window was shortened, e.g. to an hour, many of the wind components with largest background departures would be rejected. This would seem to suggest that it is useful to test a shorter assimilation window.

Mid-latitude cyclones, such as the storm of interest, are associated with high wind speeds. It is therefore essential to be able to model the ocean surface winds accurately.

In this storm event, the model background winds were always higher than the assimilated scatterometer winds when background wind speeds were higher than 23 m/s (Figure 6). Similar result have been found at Météo-France (*C. Payan*, personal communication, January 2015). On weak winds, the model winds tend to be lower than the scatterometer. This could indicate a problem related to the model parametrisation of boundary layer over oceans, for example, by means of non-optimal surface roughness. It is also possible that the above described timing issue creates differences between ASCAT and modelled wind, particularly on high speeds. Moreover, *Vogelzang et al.* (2011) reported that ASCAT products underestimate the true wind speed averaged over all regions based on the calibrations coefficients from the triple collocation method. In any case, the number of assimilated observations with high wind speeds were limited in this study, and longer simulation periods are needed to find out if the model winds are persistently higher than scatterometer winds on strong winds.

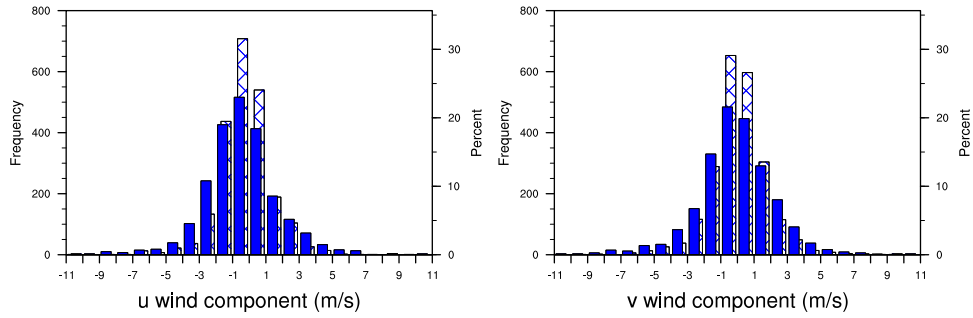


Figure 3: Frequency distribution of background departure (observation – background) and analysis departure (observation – analysis) for ASCAT zonal  $u$  and meridional  $v$  wind components (m/s) for the case Hilde-ASCAT. The blue bars indicate background departures and the hatched bars analysis departures.

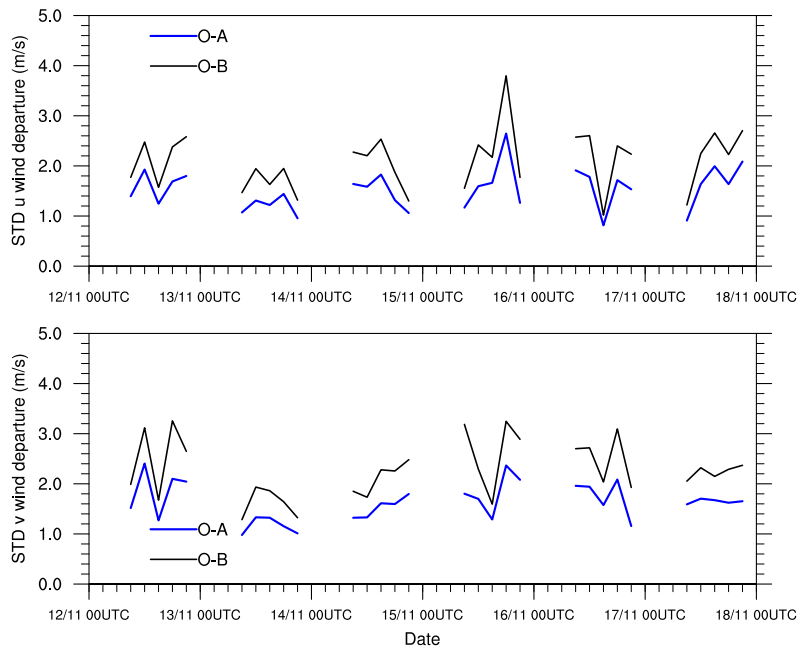


Figure 4: Time series of standard deviation of background departure (observation – background) in black, and analysis departure (observation – analysis) in blue for ASCAT zonal wind  $u$  and meridional wind  $v$  components (m/s) for the case Hilde-ASCAT.

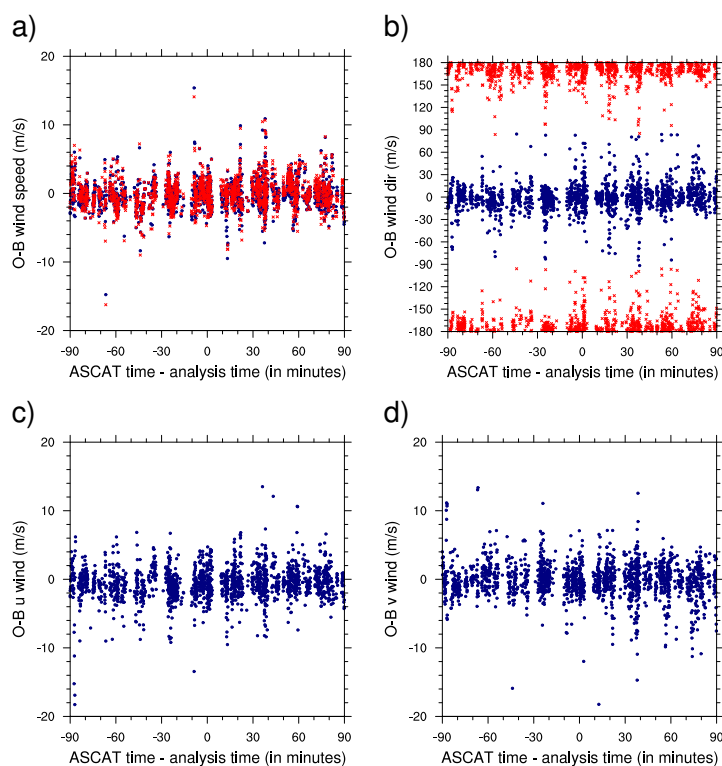


Figure 5: Scatter plot of time difference between the ASCAT measurement time and the analysis time versus HARMONIE background departure (background – observation) for a) wind speed, b) wind direction, c) zonal wind  $u$  component, and d) meridional wind  $v$  components for the case Hilde-ASCAT. The wind solutions accepted by data assimilation are marked with blue dots, and in a) and b), the wind solution rejected by the data assimilation with red crosses.

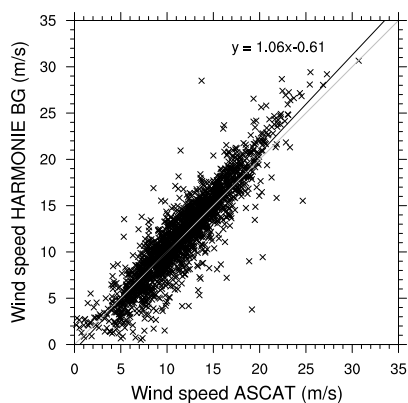


Figure 6: Scatter plot of ASCAT wind speed versus HARMONIE background wind speed (background departure - observation) for the case Hilde-ASCAT.

## 5 Impact of ASCAT data assimilation on the forecast over land

As outlined in the introduction, one of main goals of this work was to investigate the impact of scatterometer wind data assimilation on the forecasts over land. This was done by comparing the model forecasts against synoptic surface observations and vertical profiles from radiosoundings. The HARMONIE model system includes a verification package called WebgraF, which was used for calculation and plotting. Results in this section are for the experiment Hilde-ASCAT with the experiment Hilde-CONV as a control.

### 5.1 Surface variables

Impact of ASCAT data assimilation on the forecasts was assessed by evaluation of synoptic surface observations. All available synoptic surface observations were used for the evaluation. The number of stations in the evaluation is 396–536 depending on the variable and time of the day. Figure 7 presents the stations used for mean sea level pressure evaluation, and the MSLP bias (mean error) at 12UTC from all model cycles and forecast lengths. Roughly, the northern part of the domain suffers from positive MSLP bias whereas the southern part has a negative bias during the simulation period.

Figure 8 shows the surface verification for MSLP, 10-m wind speed, 2-m temperature, and 2-m specific humidity by forecast length averaged over all stations. The averaged MSLP is slightly improved by ASCAT data assimilation. Even though the impact is very small, the normalised RMSE difference between the experiments is statistically significant on forecast lengths of 3-21 hours based on Student  $t$ -test with 90% confidence level (Figures 8a-8b). Time series of 12-h forecasts (Figure 9) shows that the forecast errors are largest during the most intense storm event (16–17 November). During that time, the data assimilation of ASCAT winds improves the RMSE and bias of MSLP. This seem to suggest that ASCAT winds might have a potential to improve the forecasting of storms.

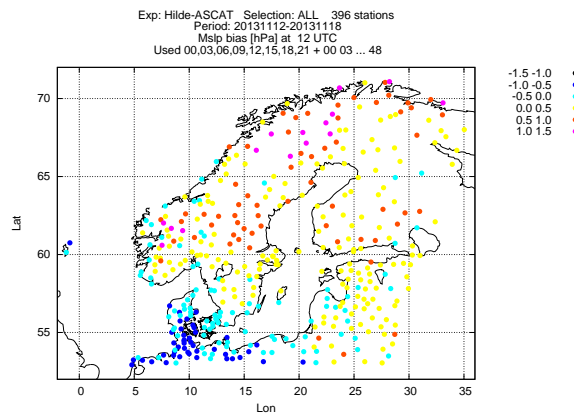


Figure 7: Station locations used for the MSLP evaluation, and MSLP bias (in colours) at 12UTC from all model cycles and forecast lengths for the case Hilde-ASCAT.

Besides MSLP surface variables do not show any statistically significant changes based on the Student  $t$ -test with 90% confidence level in normalised RMSE (Figures 8c-8h). Near surface temperature and wind fields over land, where the verification stations are located, are strongly driven locally, whereas MSLP and atmosphere well above the surface are more clearly influenced by larger scale atmospheric circulation which can be improved by scatterometer winds over oceans.

When the similar verification is done for Norwegian stations only, the results are qualitatively the same (not shown in figures). The number of stations available for verification is 56-67 depending on the variable and time of day. RMSE of MSLP, 10-m wind speed and 2-m temperature are slightly higher in Norway than the domain average whereas RMSE of 2 m specific humidity is about the same. Bias of MSLP and 2-m temperature is larger in absolute value whereas bias of 10-m wind and 2-m specific humidity is smaller in absolute value.

For the Norwegian stations, the differences of the verification scores between the experiments with and without ASCAT data are very small, and as in the domain averaged statistics, expect for the MSLP, not statistically significant based on the Student  $t$ -test with 90% confidence level in normalised RMSE. The impact of ASCAT data assimilation on MSLP is stronger in Norway than the domain average. However, the maximum impact lasts a shorter time, being 3-15 hours in forecast length. This means that during this type of westerly flow situation, scatterometer winds, measured over the ocean, have the largest impact locally over the ocean from where the impact is propagated to Norway, being highest during the short forecast lengths. The impact is further propagated along the flow resulting in longer impact length in the domain average. It is worth to keep in mind that larger amount of ASCAT data were successfully assimilated into the model system mainly twice a day, 12UTC and 18UTC. The evaluation here includes results from all model cycles.

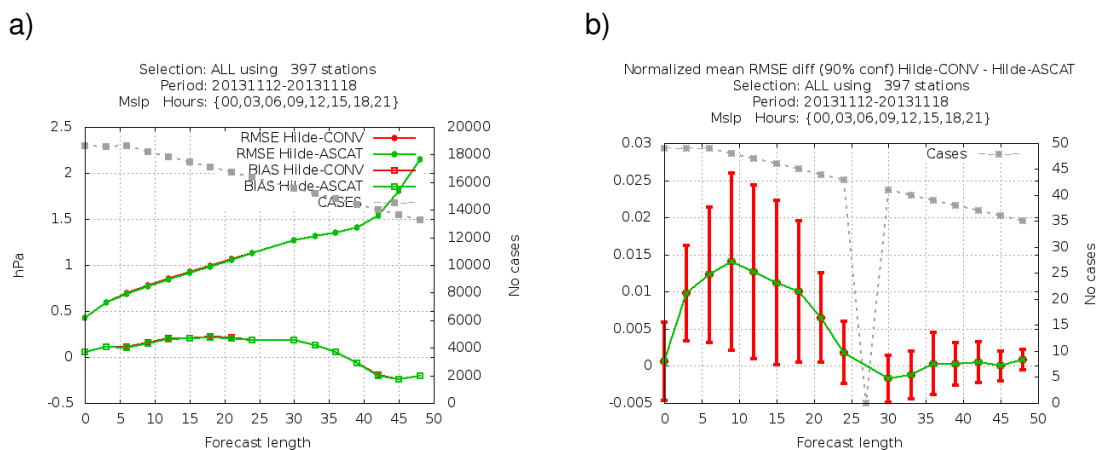


Figure 8: (Cont.)

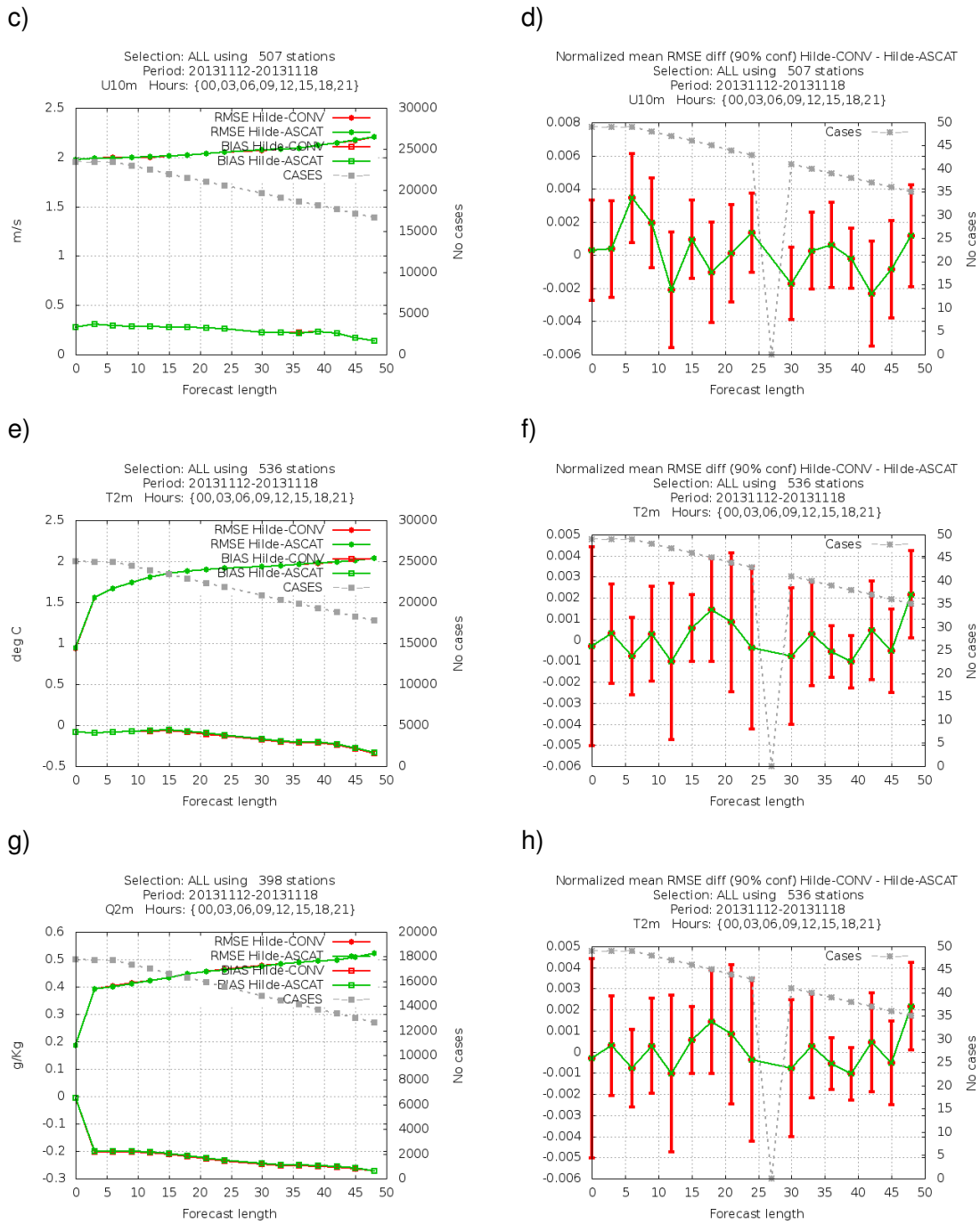


Figure 8: Mean bias (squares) and RMSE (circles) for a) MSLP, c) 10-m wind speed, e) 2-m temperature and g) 2-m specific humidity as a function of forecast length for the cases Hilde-ASCAT (green) and Hilde-CONV (red). Normalised mean RMSE difference (green) between the Hilde-ASCAT and Hilde-CONV cases for b) MSLP, d) 10-m wind speed, f) 2-m temperature and h) 2-m specific humidity. Positive values mean higher RMSE in Hilde-CONV. Red bars indicate the 90% confidence levels based on Student t-test.

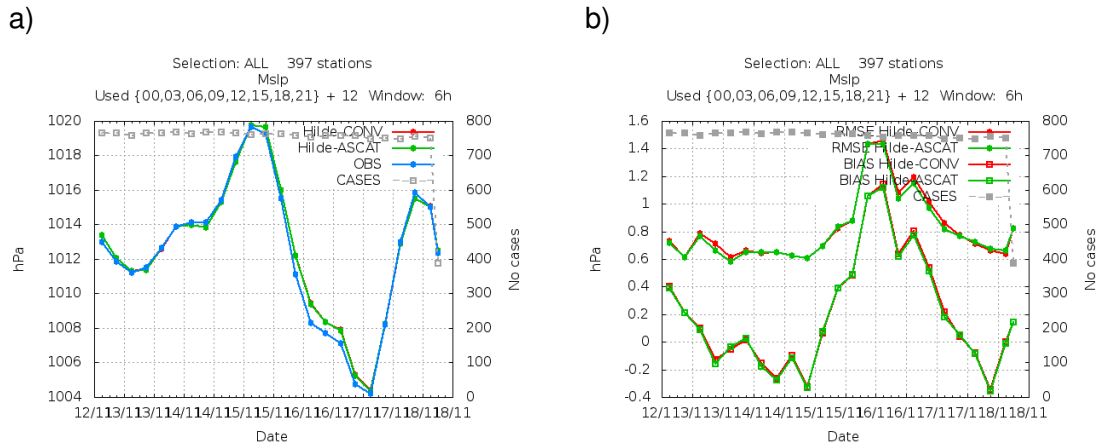


Figure 9: a) Timeseries of mean observed MSLP (blue) and 12-hour forecasts of MSLP for the cases Hilde-ASCAT (green) and Hilde-CONV (red). b) Timeseries of mean bias (squares) and RMSE (circles) of 12-hour forecasts of MSLP for the cases Hilde-ASCAT (green) and Hilde-CONV (red)

## 5.2 Upper air fields

Impact of ASCAT data assimilation on the atmospheric upper levels was assessed by evaluation of radiosounding data against the model vertical profiles. The radiosonde launches are typically done once or twice a day. There are 23 stations doing radiosoundings at 12 UTC and 19 stations at 00 UTC in the area of the model. Four of the stations are in Norway.

Figure 10 shows the verification for radiosoundings for 00UTC and 12UTC averaged over forecast lengths of 12 and 24 hours at all stations. Largest differences between the experiments with and without ASCAT data were found in the lowest and middle part of the troposphere up to 500 hPa level. However, the differences between the experiments were not consistent for each variable on different times of the day. Timeseries of each model level reveal statistically significant improvements in the 24-hour forecasts in the middle troposphere based on the Student  $t$ -test with 90% confidence level in normalised RMSE. Figure 11 shows the statistics for wind speed at 850 hPa, temperature at 700 hPa and specific humidity at 500 hPa, which showed slightly improved normalised RMSE by ASCAT data assimilation. However, wind speed bias at 850 hPa was increased. Other variables or levels did not show statistically significant improvements or degradation. The improvements demonstrate that the impact of data assimilation of ASCAT surface winds propagates into the higher model levels, and that ASCAT surface winds are able to change the dynamical development of upper structures at least in some extent. Similar results are also seen in the global ECMWF model system, where scatterometer observations have found to have an impact up to 600 hPa in the full model system with all

observations assimilated (*De Chiara et al.*, 2014). In a single observation experiment with only scatterometer wind assimilation, *De Chiara et al.* (2014) found the largest analysis increments around 850 hPa with visible increments up to 100 hPa. In the Arpège global model of Météo-France, the scatterometer winds have shown to have a positive impact at the higher levels (pressure lower than 300 hPa) (*Payan*, 2008).

Longer study periods are needed to find out the impact of ASCAT winds on higher levels of atmosphere in general and in Norway.

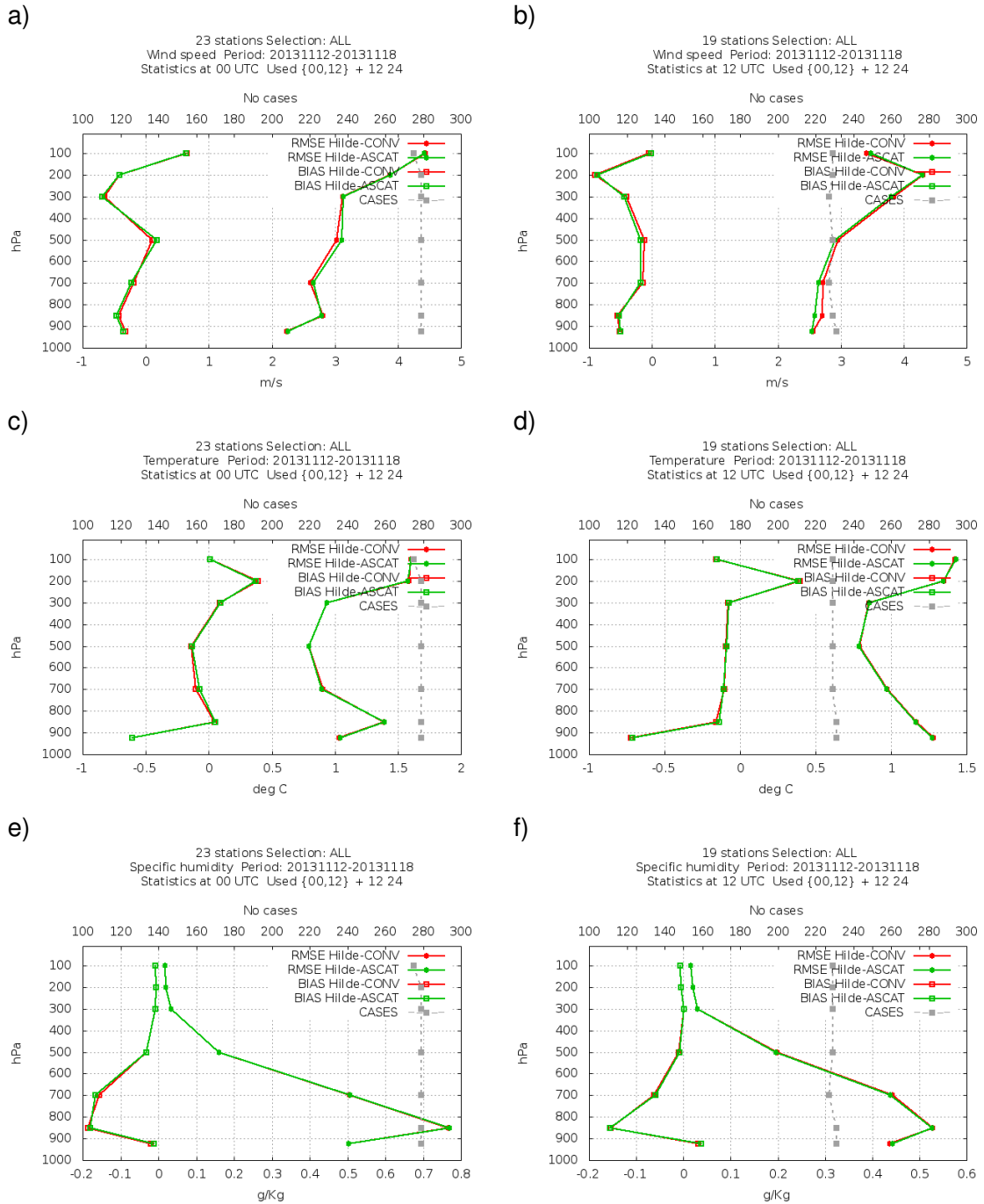


Figure 10: Mean bias (squares) and RMSE (circles) for a) and b) wind speed, c) and d) temperature, and e) and f) specific humidity at 00UTC and 12 UTC, respectively, averaged over forecast lengths of 12 hours and 24 hours for the cases Hilde-ASCAT (green) and Hilde-CONV (red).

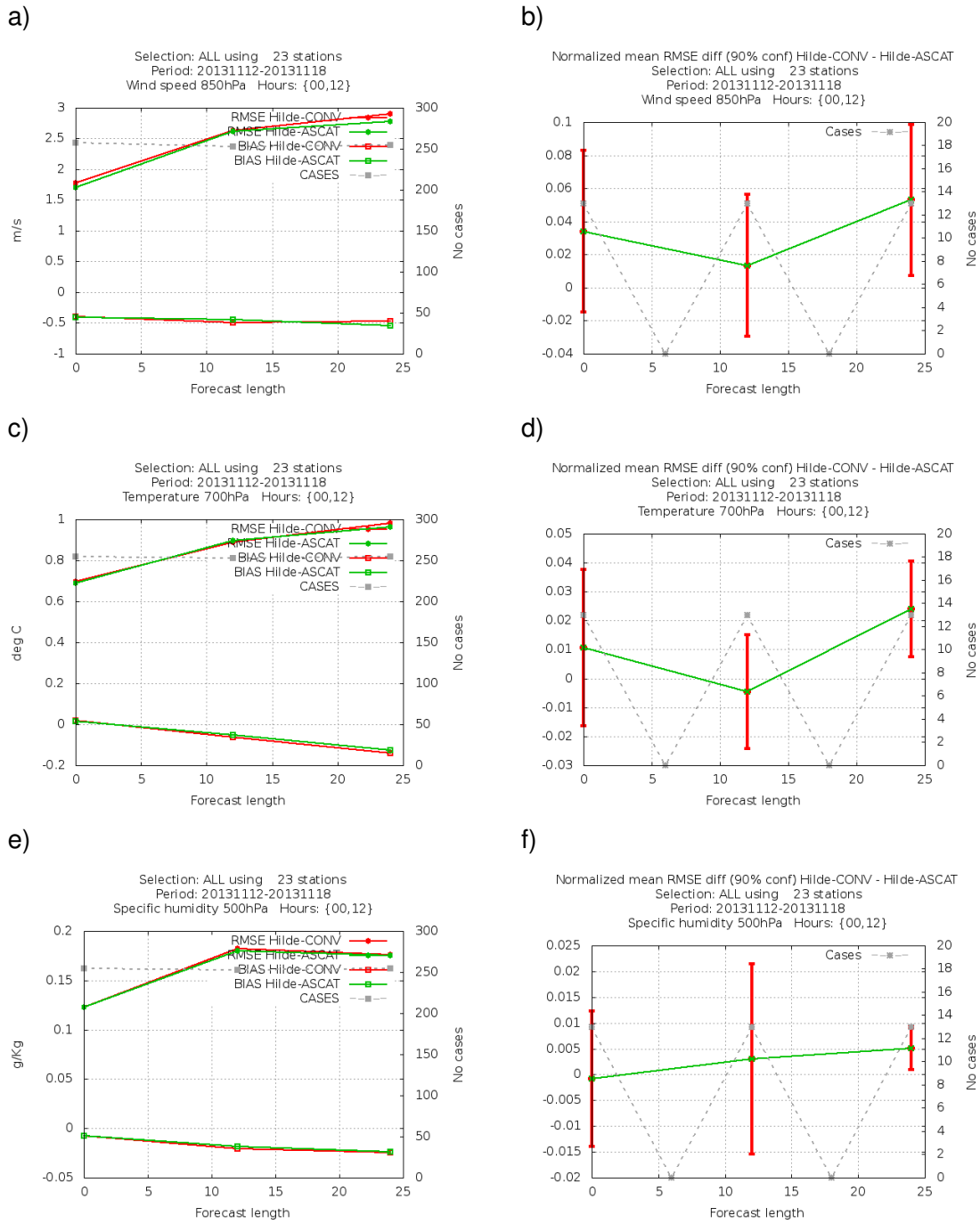


Figure 11: Mean bias (squares) and RMSE (circles) for a) wind speed at 850 hPa, c) temperature at 700 hPa and e) specific humidity at 500 hPa as a function of forecast length for the cases Hilde-ASCAT (green) and Hilde-CONV (red). Normalised mean RMSE difference (green) between the Hilde-ASCAT and Hilde-CONV cases for b) wind speed at 850 hPa, d) temperature at 700 hPa, and f) specific humidity at 500 hPa. Positive values mean higher RMSE in Hilde-CONV. Red bars indicate the 90% confidence levels based on Student *t*-test.

## 6 Test on the reduced thinning distance

It has been argued that the thinning distance of 100 km for ASCAT wind data could be reduced. To test this, the thinning distance was reduced to 50 km. Other settings were kept the same. The settings with reduced thinning was applied for the cyclone case (Hilde-ASCATthinn) and for the polar low case (PL-ASCATthinn). The results from both experiments are shown in this section.

When reducing the thinning distance, the amount of data that was used in the data-assimilation was then clearly larger, leading to 6% of the data being used at the end. Background departure statistics showed marginal differences compared to the default thinning (Figure 12). Mean standard deviations (2.25 m/s and 2.48 m/s for  $u$  and  $v$ ) were slightly increased. Analysis departures, on the contrary, were clearly smaller (1.29 m/s and 1.43 m/s for  $u$  and  $v$ ). Figure 13 shows the time evolution of standard deviations of the departures demonstrating that the ASCAT observations had been given more weight in this case. The ambiguity selection problems close to fronts described above were also common in these experiments.

Impact evaluation on the surface stations showed that reduced thinning gives further marginally improved forecasts of MSLP on short forecast lengths (Figure 14). Although, the RMSE of MSLP as well as RMSE of temperature at 700 hPa at the analysis time were slightly higher with reduced thinning. Other surface variables showed no statistically significant improvements based on Student  $t$ -test with 90% confidence level, but no degradation either. This indicates that it might be beneficial to reduce the thinning distance to 50 km. Nevertheless, more experimentation is needed to see if the benefit is consistent over time, and to make sure observations are not weighted too much.

The settings with increased thinning leads to giving more weight to the observations. However, we cannot know whether the larger number of observations is adding any useful features, or they are compensating for a possible mistuning of the ratio of observation errors and the background errors. This is planned to be checked by comparing a simulation with reduced thinning and no change in observation error to an simulation with default thinning and reduced observation error variance. If the reduced thinning distance really gives a better result than simply adjusting the observation error, it would be an indication that the assimilation system can digest the increased resolution in the observations. Otherwise it is more an indication that the weighting is not optimal for the case in question.

The experimental setup with reduced thinning distance of 50 km was then applied into a case with high polar low activity in the Barents Sea. Standard deviations of background departures of the used ASCAT winds (Figure 15) were larger than in the cyclone case. This illustrates the large flow dependent variations associated with different meteorological events.

The slight improvements in verification scores of MSLP were not statistically significant averaged over the whole simulation period (Figure 16). When focusing on the time when the polar low was moving within the domain, substantial improvement was achieved

on MSLP bias and RMSE (Figure 17). For Norwegian stations only, the impact is larger (not shown in figures), though not statistically significant. It should, however, be noted that the surface pressure field at the time was strongly influenced by a larger scale low pressure in the Atlantic, which may have dominated the statistics. In the future, care should be taken to limit the region of study in order to investigate the impact on polar lows only. Nevertheless, the results indicate improvements in MSLP for this case, and seem to support the idea that scatterometer wind assimilation might be beneficial for forecasting of polar lows on high-resolution NWP.

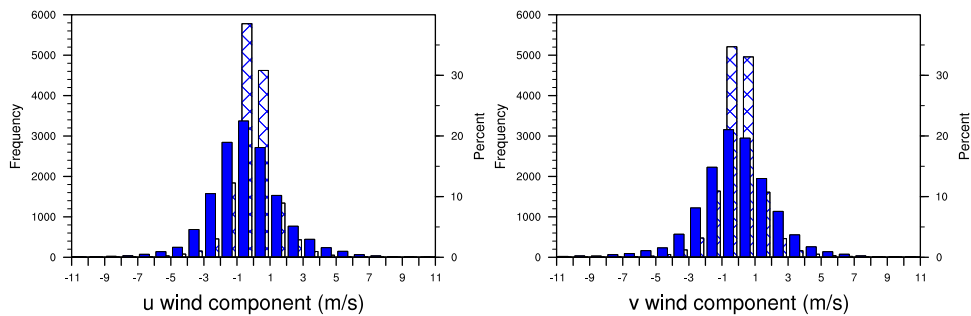


Figure 12: As Figure 3 but for the case Hilde-ASCATthinn

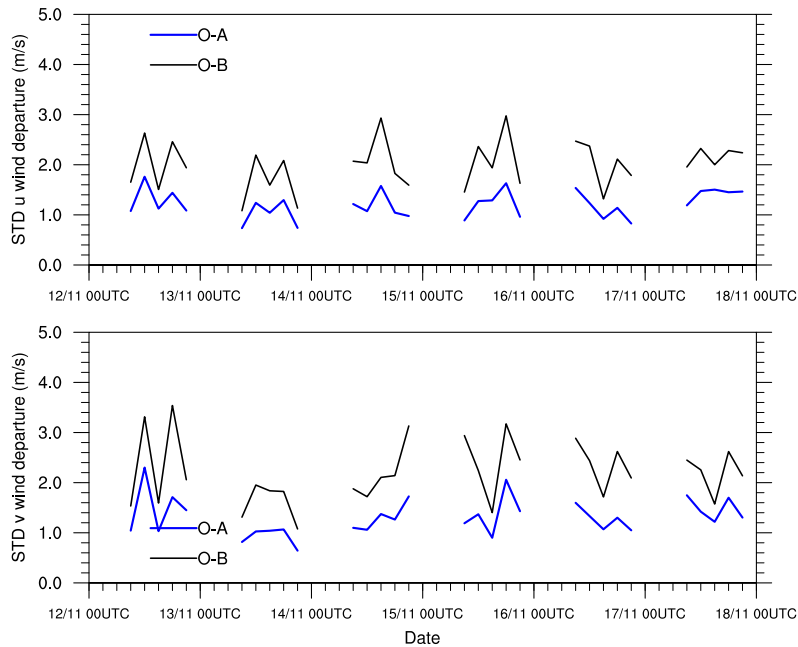
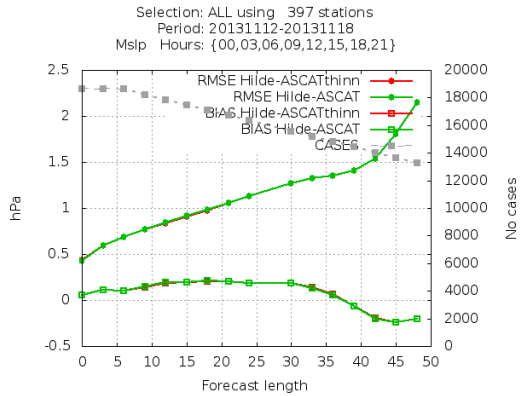


Figure 13: As Figure 4 but for the case Hilde-ASCATthinn.

a)



b)

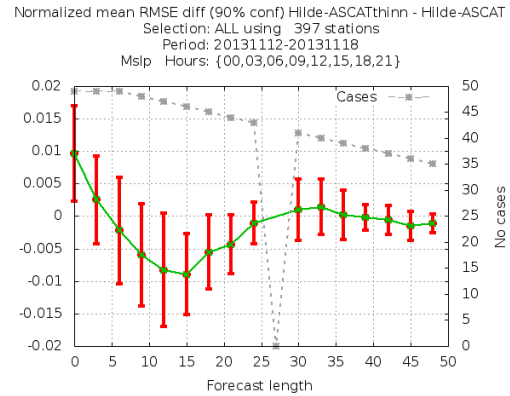


Figure 14: a) Mean bias (squares) and RMSE (circles) for MSLP as a function of forecast length for the cases Hilde-ASCAT (green) and Hilde-ASCATthinn (red). b) Normalised mean RMSE difference (green) between the Hilde-ASCAT and Hilde-ASCATthinn cases for MSLP. Positive values mean higher RMSE in Hilde-ASCATthinn. Red bars indicate the 90% confidence levels based on Student *t*-test.

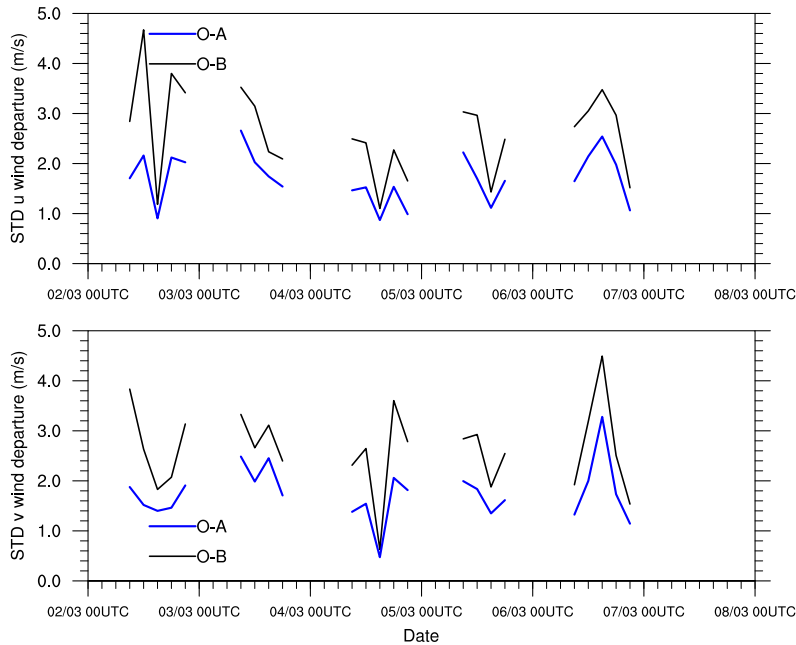


Figure 15: As Figure 4 but for the case PL-ASCATthinn.

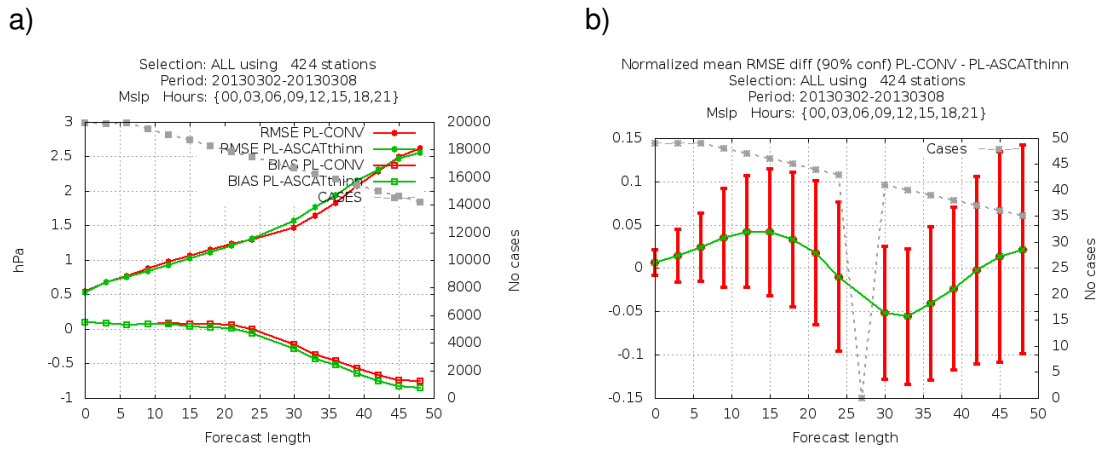


Figure 16: a) Mean bias (squares) and RMSE (circles) for MSLP as a function of forecast length for the cases PL-ASCATthinn (green) and PL-CONV (red). b) Normalised mean RMSE difference (green) between the PL-ASCATthinn and PL-CONV cases for MSLP. Positive values mean higher RMSE in PL-CONV. Red bars indicate the 90% confidence levels.

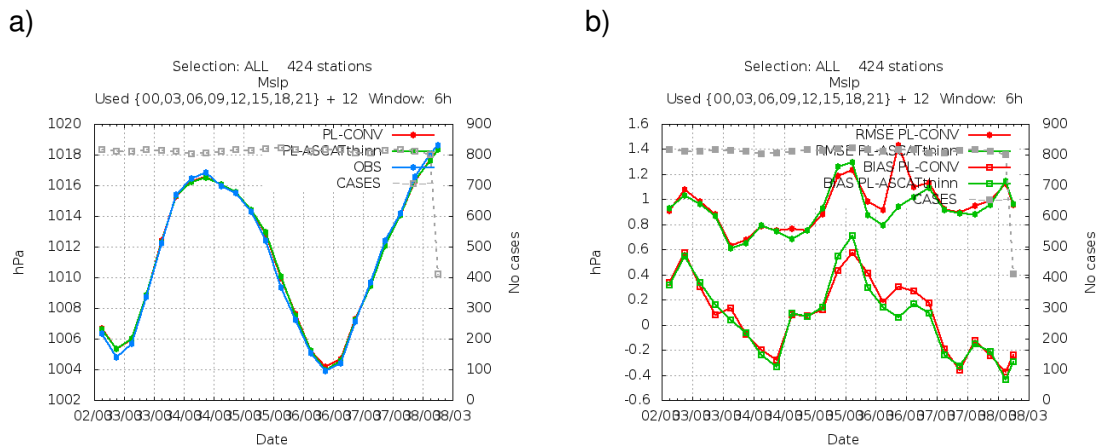


Figure 17: a) Timeseries of mean observed MSLP (blue) and 12-hour forecasts of MSLP for the cases PL-ASCATthinn (green) and PL-CONV (red). b) Timeseries of mean bias (squares) and RMSE (circles) of 12-hour forecasts of MSLP for the cases PL-ASCATthinn (green) and PL-CONV (red).

## 7 Conclusions and outlook

The fellowship project SCARASTO aims to take better benefit of scatterometer winds in situations of rapidly developing storms. During the first year of the project, skills in the implementation and available settings of scatterometer assimilation in the HARMONIE model system were achieved. Data from MetOp-A and MetOp-B satellites were applied in the 3D-Var data assimilation system for selected storm cases. Coverage, quality and impact of ASCAT data were studied.

The ASCAT wind data assimilation was found to give a slight positive impact on the forecasts of mean sea level pressure on forecast lengths of 3-21 hours in a severe cyclone case. In the upper levels of atmosphere, it was obtained a slight improvement on the RMSE of the 24-h forecast of wind speed at 850 hPa, temperature at 700 hPa and specific humidity at 500 hPa. There was no statistically significant impact on other surface or upper atmosphere variables found. As the average scores are barely influenced by ASCAT data, in the future more focus should be put on those forecast cycles when the ASCAT data is available.

The presently applied ASCAT assimilation in HARMONIE is based on an initial configuration not believed to be optimal for the present resolution and configuration of the model. The first attempt to optimise the use of ASCAT winds was done by reducing the thinning distance. In the cyclone case, slightly improved average verification scores for MSLP were obtained with reduced thinning of ASCAT data. When reduced thinning was applied to a polar low case, standard deviations of background departures were larger than in the cyclone case. Statistically significant improvements were not obtained on scores averaged over the longer period, but a clear improvement was made at the time of the polar low event.

The difference between the observation and the model analysis time induces departures between the ASCAT winds and the model, and limits the impact of ASCAT winds in the analysis. In the current model system with 3D-Var, the found ambiguity selection problems near to proceeding fronts could be decreased with a shorter assimilation window and that work is ongoing.

Another factor limiting the impact from scatterometer data is the description of background error covariances. The current settings make use of static background error covariance (**B** matrix) based on averaged structures, which is not optimal for the storm cases. Revisiting the background-error estimation might help to improve the impact of ASCAT winds. The four-dimensional variational (4D-Var) data assimilation method in the HARMONIE system is close to being available for testing. 4D-Var assimilation would likely reduce the problem of ambiguity selection as well as the issues rising from the static background errors.

Even though improvements were achieved with the use of ASCAT data in the studied cases, the findings cannot be generalised. More experimentation is clearly needed. Nevertheless, the prospect of being able to improve the forecasting of severe storms, serves as an incentive for further ongoing research within the fellowship project.

## Acknowledgements

Teresa Valkonen's work at MET Norway is funded by the EUMETSAT Fellowship Programme. KNMI is acknowledged for providing the archived ASCAT data. The authors greatly appreciate the help of Gert-Jan Marseille (KNMI), Christophe Payan (Météo-France), and the HIRLAM colleagues who have made it possible to work with the HARMONIE model system.

## References

ASCAT Wind Product User Manual (2013), Ocean and Sea Ice SAF version 1.13, reference: SAF/OSI/CDOP/KNMI/TEC/MA/126.

Berre, L. (2000), Estimation of synoptic and mesoscale forecast error covariances in a limited-area model, *Mon. Wea. Rev.*, *128*, 644–667.

Brousseau, P., L. Berre, F. Bouttier, and G. Desroziers (2011), Background-error covariances for a convective-scale data-assimilation system: AROME-France 3D-Var, *Q.J.R. Meteorol. Soc.*, *137*, 409–422, doi: 10.1002/qj.750.

Cotton, J. (2013), The impact of ASCAT winds from Metop-B and a new scatterometer thinning scheme, *Forecasting Research Technical Report No. 580*, Met Office, available at <http://www.metoffice.gov.uk/learning/library/publications/>.

Cuxart, J., P. Bougeault, and J.-L. Redelsperger (2000), A turbulence scheme allowing for mesoscale and large-eddy simulations, *Q.J.R. Meteorol. Soc.*, *126*, 1–30, doi: 10.1002/qj.49712656202.

Dahlgren, P. (2013), A Comparison Of Two Large Scale Blending Methods – Jk and LSMIXBC, *MetCoOp Technical Memorandum, 2/2013*, The Norwegian Meteorological Institute and Swedish Meteorological and Hydrological Institute, available at <http://metcoop.org/memo>.

De Chiara, G., P. Janssen, H. Hersbach, and N. Bormann (2012), Assimilation of scatterometer winds at ECMWF, *Proceedings of the 11th International Winds Workshop, Auckland, New-Zealand, 20-24 February 2012*, EUMETSAT, available at <http://www.eumetsat.int/>.

De Chiara, G., P. Janssen, S. English, J.-R. Bidlot, and P. Laloyaux (2014), Scatterometer impact studies at ECMWF, *Proceedings of the EUMETSAT Meteorological Satellite Conference, Geneva, Switzerland, 22-26 September 2014*, EUMETSAT, available at <http://www.eumetsat.int/>.

de Haan, S., G.-J. Marseille, P. de Valk, and J. de Vries (2013), Impact of ASCAT Scatterometer Wind Observations on the High-Resolution Limited-Area Model

- (HIRLAM) within an Operational Context, *Wea. Forecasting*, 28, 489–503, doi: <http://dx.doi.org/10.1175/WAF-D-12-00056.1>.
- de Rooy, W. C., and A. Pier Siebesma (2010), Analytical expressions for entrainment and detrainment in cumulus convection, *Q.J.R. Meteorol. Soc.*, 136, 1216–1227, doi: 10.1002/qj.640.
- Derber, J., and F. Bouttier (1999), A reformulation of the background error covariance in the ECMWF global data assimilation system, *Tellus A*, 51, 195–221, doi: 10.1034/j.1600-0870.1999.t01-2-00003.x.
- Ekstremvêrappport (2013), Hending: Hilde, 16.-17.11.2013. [Report of extreme weather event: Case Hilde 16-17 November 2013.], *MET info no. 15/2013*, the Norwegian Meteorological Institute, Bergen.
- Figa-Saldaña, J., J. Wilson, E. Attema, R. Gelsthorpe, M. Drinkwater, and A. Stoffelen (2002), The advanced scatterometer (ASCAT) on the meteorological operational (MetOp) platform: A follow on for European wind scatterometers, *Can. J. Remote Sensing*, 28(3), 404–412.
- Gilbert, J., and C. Lemaréchal (1989), Some numerical experiments with variable-storage quasi-Newton algorithms, *Mathematical Programming*, 45, 407–435.
- Hersbach, H., A. Stoffelen, and S. de Haan (2007), An improved C-band scatterometer ocean geophysical model function: CMOD5, *J. Geophys. Res.*, 112(C3), doi: 10.1029/2006JC003743, c03006.
- Lin, W., M. Portabella, A. Stoffelen, and A. Verhoef (2013), On the characteristics of ascats wind direction ambiguities, *Atmospheric Measurement Techniques*, 6(4), 1053–1060, doi:10.5194/amt-6-1053-2013.
- Masson, V., P. Le Moigne, E. Martin, S. Faroux, A. Alias, R. Alkama, S. Belamari, A. Barbu, A. Boone, F. Bouyssel, P. Brousseau, E. Brun, J.-C. Calvet, D. Carrer, B. Decharme, C. Delire, S. Donier, K. Essaouini, A.-L. Gibelin, H. Giordani, F. Habets, M. Jidane, G. Kerdraon, E. Kourzeneva, M. Lafaysse, S. Lafont, C. Lebeaupin Brossier, A. Lemonsu, J.-F. Mahfouf, P. Marguinaud, M. Mokhtari, S. Morin, G. Pigeon, R. Salgado, Y. Seity, F. Taillefer, G. Tanguy, P. Tulet, B. Vincendon, V. Vionnet, and A. Voldoire (2013), The surfexv7.2 land and ocean surface platform for coupled or offline simulation of earth surface variables and fluxes, *Geoscientific Model Development*, 6(4), 929–960, doi:10.5194/gmd-6-929-2013.
- Mlawer, E. J., S. J. Taubman, P. D. Brown, M. J. Iacono, and S. A. Clough (1997), Radiative transfer for inhomogeneous atmospheres: RRTM, a validated correlated-k model for the longwave, *J. Geophys. Res.*, 102(D14), 16,663–16,682, doi:10.1029/97JD00237.

- Morcrette, J.-J., and Y. Fouquart (1986), The Overlapping of Cloud Layers in Shortwave Radiation Parameterizations, *J. Atmos. Sci.*, 43, 321–328, doi: [http://dx.doi.org/10.1175/1520-0469\(1986\)043<0321:TOOCLI>2.0.CO;2](http://dx.doi.org/10.1175/1520-0469(1986)043<0321:TOOCLI>2.0.CO;2).
- Noer, G., Ø. Sætra, T. Lien, and Y. Gusdal (2011), A climatological study of polar lows in the Nordic Seas, *Quarterly Journal of the Royal Meteorological Society*, 137(660), 1762–1772, doi:10.1002/qj.846.
- Ollinaho, P. (2010), Feasibility of assimilating ASCAT surface winds into a limited area, Master's thesis, Dept. of Physics, University of Helsinki, available at <https://helda.helsinki.fi/bitstream/handle/10138/20968/feasibil.pdf>.
- Payan, C. (2008), Status of the use of scatterometer data at Météo-France, *Proceedings of the 9th International Winds Workshop, Annapolis, Maryland, USA, 14-18 April 2008*, EUMETSAT, available at <http://www.eumetsat.int/>.
- Payan, C. (2010), Improvements in the use of scatterometer winds in the operational NWP system at Météo-France, *Proceedings of the 10th International Winds Workshop, Tokyo, Japan, 22-26 February 2010*, EUMETSAT, available at <http://www.eumetsat.int/>.
- Payan, C. (2012), Satellite winds activities at Météo-France, *Proceedings of the 11th International Winds Workshop, Auckland, New-Zealand, 20-24 February 2012*, EUMETSAT, available at <http://www.eumetsat.int/>.
- Pinty, J.-P., and P. Jabouille (1998), A mixed-phased cloud parameterization for use in a mesoscale non-hydrostatic model: Simulations of a squall line and of orographic precipitation, *Proc. Conf. of Cloud Physics, Everett, WA, USA, Amer. Meteor. soc., Aug. 1999*, pp. 217–220.
- Plan for varsling av ekstreme værforhold (2014), Oppdatert 9.april 2014. [Plan for the prediction of extreme weather conditions. Updated 9 April, 2014], *The Norwegian Meteorological Institute*.
- Seity, Y., P. Brousseau, S. Malardel, G. Hello, P. Bénard, F. Bouttier, C. Lac, and V. Masson (2011), The AROME-France Convective-Scale Operational Model, *Mon. Wea. Rev.*, 139, 976–991, doi: <http://dx.doi.org/10.1175/2010MWR3425.1>.
- Stoffelen, A. (1998), Scatterometry, *PhD Thesis*, University of Utrecht, the Netherlands.
- Taillefer, F. (2002), CANARI - Technical Documentation - Based on ARPEGE cycle CY25T1 (AL25T1 for ALADIN), *Météo-France*, available at <http://www.cnrm.meteo.fr/aladin/>.
- Tveter, F. T. (2006), Assimilating ambiguous QuikScat scatterometer observations in HIRLAMF 3-D-Var at the Norwegian Meteorological Institute, *Tellus A*, 58(1), 59–68, doi:10.1111/j.1600-0870.2006.00155.x.

- Ulaby, F. T., R. K. Moore, and A. Fung (1982), *Microwave Remote Sensing: Active and Passive, Vol. II – Radar Remote Sensing and Surface Scattering and Emission Theory*, 609 pp., Addison-Wesley, Advanced Book Program, Reading, Massachusetts.
- Verhoef, A., M. Portabella, A. Stoffelen, and H. Hersbach (2008), CMOD5.n - the CMOD5 GMF for neutral winds, *OSI SAF report*, SAF/OSI/CDOP/KNMI/TEC/TN/165.
- Verspeek, J., M. Portabella, A. Stoffelen, and A. Verhoef (2013a), ASCAT Calibration and Validation, *OSI SAF Technical report*, SAF/OSI/CDOP/KNMI/TEC/TN/163.
- Verspeek, J., A. Verhoef, and A. Stoffelen (2013b), ASCAT-B NWP Ocean Calibration and Validation, *OSI SAF Technical report*, SAF/OSI/CDOP2/KNMI/TEC/RP/199.
- Vogelzang, J., A. Stoffelen, A. Verhoef, J. de Vries, and H. Bonekamp (2009), Validation of two-dimensional variational ambiguity removal on sea-winds scatterometer data, *J. Atmos. Oceanic Technol.*, 26, 1229–1245, doi: <http://dx.doi.org/10.1175/2008JTECHA1232.1>.
- Vogelzang, J., A. Stoffelen, A. Verhoef, and J. Figa-Saldaña (2011), On the quality of high-resolution scatterometer winds, *Journal of Geophysical Research: Oceans*, 116(C10), doi:10.1029/2010JC006640.

## Appendix: List of abbreviations and acronyms

3D-Var	Three-Dimensional Variational data assimilation
4D-Var	Four-Dimensional Variational data assimilation
ALADIN	Aire Limitée Adaptation dynamique Développement InterNational
AIREP	AIRcraft REPorts
AMDAR	Aircraft Meteorological DATA Relay Observations
AR	Ambiguity removal
ASCAT	Advanced SCATterometer
CANARI	Code d'Analyse Nécessaire à Arpege pour ses Rejets et son Initialisation
DRIBU	Drifted buoy
EARS	EUMETSAT Advanced Retransmission Service
ECMWF	European Centre for Medium-Range Weather Forecasts
EPS	EUMETSAT Polar System
ESA	European Space Agency
EUMETSAT	European Organisation for the Exploitation of Meteorological Satellites
FGAT	First Guess at Appropriate Time
GMF	Geophysical Model Function
HARMONIE	Hirlam Aladin Regional/Meso-scale Operational NWP In Europe
HIRLAM	High Resolution Limited Area Model
KNMI	Royal Netherlands Meteorological Institute
MET Norway	Norwegian Meteorological Institute
MetOp	Meteorological Operational EPS satellite
MLE	Maximum Likelihood Estimator
MSLP	Mean sea level pressure
NRCS	Normalised radar cross section
NWP	Numerical Weather Prediction
OSI SAF	Ocean and Sea Ice Satellite Application Facility
RMSE	Root mean square error
SCARASTO	Scatterometer winds in rapidly developing storms
SHIP	Synoptic observations from ships
STD	Standard deviation
SURFEX	SURFace EXternalisée, a surface model
SYNOP	Surface synoptic observations
TEMP	Upper air soundings
UTC	Coordinated Universal Time
WVC	Wind vector cell

